

# Novel Multistable Corrugated Structures

Alex D. Norman,<sup>\*</sup> Simon D. Guest<sup>†</sup> and Keith A. Seffen<sup>‡</sup>

*Cambridge University, Engineering Department, Trumpington Street, Cambridge, CB2 1PZ, UK*

We have been investigating the properties, behaviour and stability of multistable open corrugated shells. This multistability arises from the interaction between internal prestresses created during forming and non-linear geometrical changes during deformation. Two modes of bistability are described here: prestressed corrugated shells which, when buckled, can coil up into a tube repeatedly and reversibly, and corrugated sheets with a global cylindrical curvature, which is stable in either of two symmetric directions. Both modes can be present at the same time, creating a tristable shell. Using simplified analytical elastic models, we homogenise the properties of the shells through simultaneously considering the material on two scales: the ‘local’ scale of the isotropic material and the ‘global’ scale of the corrugated sheet, which is then modelled as a homogenised, flat, anisotropic sheet. The models produce similar behaviour to our prototypes, and have taught us how to incorporate or eradicate the various modes at will. The insights and methods developed from these simple models are paving the way to developing more complex corrugated forms with even more general and interesting shape-changing characteristics.

## Nomenclature

$\theta$	Angle (degrees $^{\circ}$ )
$\kappa$	Curvature ( $\text{m}^{-1}$ )
$\lambda$	Corrugation wavelength (m)
$\nu$	Poisson’s ratio
$a$	Corrugation amplitude at a point, measured from the mid-plane of the corrugated sheet
$c$	Corrugation curvature ( $\text{m}^{-1}$ )
$t$	Local shell thickness
$D$	Bending stiffness (N m)
$E$	Young’s Modulus ( $\text{N m}^{-2}$ )
$M$	Bending moment per unit length (N)
$U$	Energy per unit area ( $\text{N m}^{-1}$ )
<i>Subscripts &amp; superscripts</i>	
$\hat{()}$	Dimensionless property
$\overline{()}$	Mean average over the material area/length
$()_{\text{M}}$	Value at a local energy minimum (i.e. a stable point)

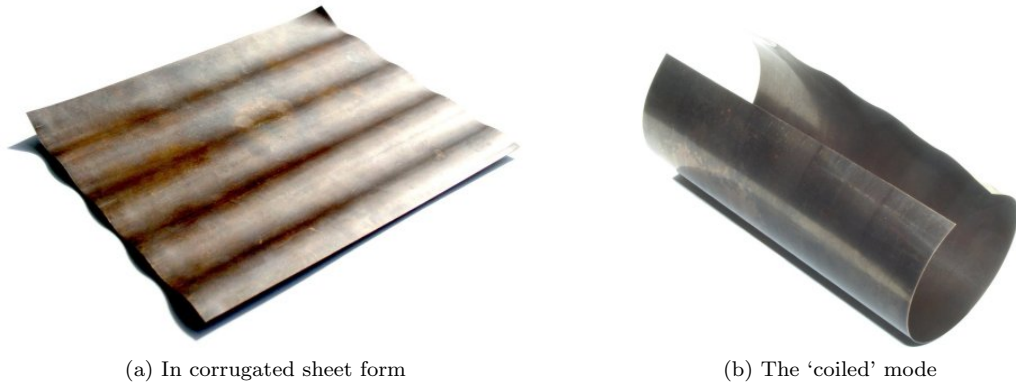
## I. Introduction

FIGURE 1 shows a simple bistable corrugated shell, originally conceived by Dr Keith Seffen. One stable state (Figure 1a) is a globally flat sheet of uniform, circular-arc corrugations. This state is not unstressed; there are stresses within (which we term initial stresses, or ‘prestresses’) which are attempting to coil the sheet. If part of the shell is manually flattened across the corrugations, these stresses are released, and the sheet ‘coils up’ rapidly into the state of Figure 1b. The shell can be repeatedly and reversibly ‘snapped’ between the two states; at no point is the deformation plastic.

<sup>\*</sup>PhD candidate, Structures Group, University of Cambridge Department of Engineering.

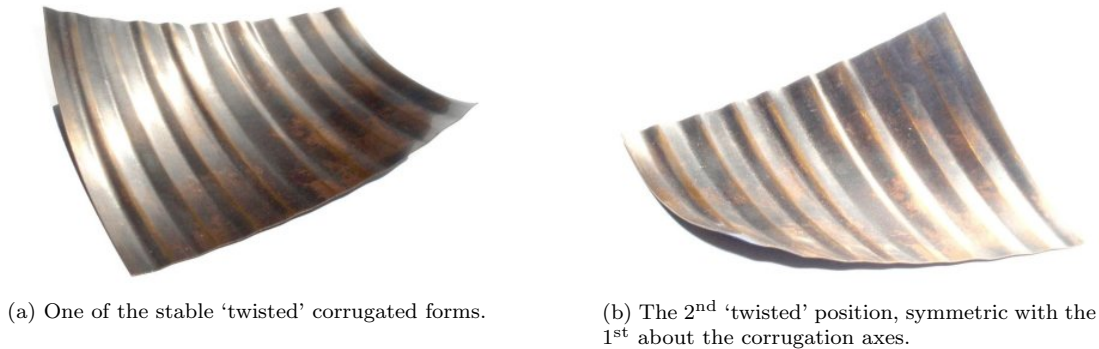
<sup>†</sup>Reader in Structural Mechanics, Structures Group, University of Cambridge Department of Engineering.

<sup>‡</sup>University Lecturer in Engineering, Structures Group, University of Cambridge Department of Engineering.



(a) In corrugated sheet form (b) The ‘coiled’ mode

Figure 1: A typical bistable shell. A bending prestress is held in equilibrium by the moment arm of the membrane stresses in the corrugated sheet (left): when the corrugations are elastically flattened, the prestresses are released and the sheet coils up.



(a) One of the stable ‘twisted’ corrugated forms. (b) The 2<sup>nd</sup> ‘twisted’ position, symmetric with the 1<sup>st</sup> about the corrugation axes.

Figure 2: The two ‘twisted’ corrugated stable states of a typical tristable shell. These stable states are in fact a cylindrical curvature of the corrugated sheet about an axis not aligned with the corrugations.

Early prototypes produced unexpected ‘twisting’ corrugated modes, making the sheets tristable, albeit no longer globally flat. This is shown in Figure 2. The single corrugated mode has now split into two corrugated modes of equal global curvature. This curvature can take any direction depending upon the construction of the shell, and the two modes are symmetric about the corrugations. Furthermore, these two modes can be combined in one shell, creating a tristable shell with two twisted, corrugated modes and one coiled mode.

### I.A. Motivation

Conventional structures are designed to maintain a single shape throughout their design life, across the range of loadings. Where a machine has to move to fulfil its function, we see a series of such structures connected by hinges, linkages, sliders, bearings &c. both to provide and to constrain the degrees of freedom, then being directed by actuators, resulting in a complex system, requiring lubrication and maintenance. On the other hand, a multistable structure can undergo large changes of shape without hinges or any such mechanisms, and yet (by definition of multistability) can ‘lock’ safely into various shapes, giving the potential for large improvements in cost, weight, complexity, reliability and lifespan. Specifically, a *corrugated* shell structure can combine light weight with high strength, offering a wide scope for the designer to tailor the stiffness properties to the required behaviour.

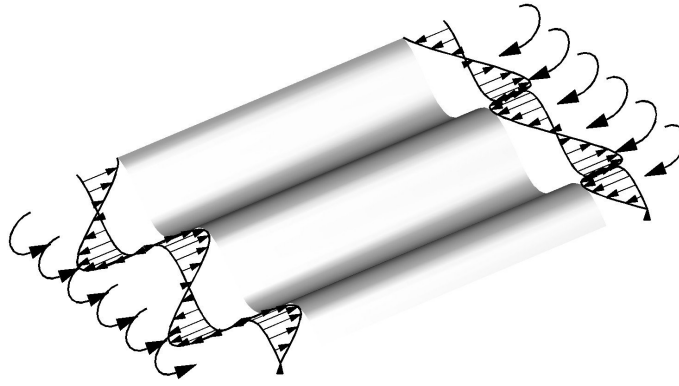


Figure 3: How prestresses are sustained in equilibrium. The circular arrows show the direction of a uniform shell bending moment caused by internal stresses, i.e. the ‘prestress’. Linear arrows show the distribution of membrane stresses, which vary across the corrugations, and so equilibrium is maintained.

## I.B. Background

Much has been written on the elastic & plastic theory of thin shells. For the former, a good basic understanding comes from a book by Calladine.<sup>1</sup> However, general analytical solutions for the large-deflection elastic or plastic behaviour of corrugated shells have yet to be found. We have traced work on multistable shells back to Hyer in 1981,<sup>2</sup> who observed the shapes assumed at room temperature by asymmetric composite laminates that had been cured at elevated temperatures. Rather than the saddle shape predicted by small-deflection linear theory, the laminates assumed one of two approximately cylindrical curvatures.

Guest & Pellegrino<sup>3</sup> have extended matters to consider *initially* cylindrically-curved shells, showing that all interesting behaviour can be considered as inextensional, since the bending of a thin shell involves significantly less energy input than the stretching required for rendering double curvature of similar magnitude. Importantly, twisting curvatures must be considered in stability calculations, as Galletly & Guest show.<sup>4</sup>

The above concern composites; isotropic shells are studied by Kebabze et. al.,<sup>5</sup> again considering simple cylindrical curvatures. However, it is found that unlike anisotropic composite shells, cylindrically-curved isotropic shells cannot display multistability without some prestress.

## II. Qualitative theory & explanation

A simple explanation of how multistability functions and is created is given below. Inevitably, it echoes the explanation of prestress & multistability in isotropic shells found in Kebabze et. al.,<sup>5</sup> although here the situation is elaborated, by dealing with corrugated shells rather than uniformly curved shells.

### II.A. How prestresses enable multistability in isotropic materials

Figure 3 shows the effect of prestress, and how multistability arises. In the initial (corrugated, globally flat) shape, there are residual stresses within the shell which exert a bending moment along the corrugations, denoted in Figure 3 by circular arrows. The corrugated sheet does not coil up because these bending stresses are held in equilibrium by the distribution of membrane stresses. Flattening the corrugations causes all membrane stresses to lie in a single plane. Now, they exert no moment, and nothing resists the prestress; thus, the shell coils up.

The existence of membrane stresses in the corrugated state implies some stretching and compression in the corrugated shell, which leads to another way of thinking about multistability: the corrugations move material away from the centreplane of the shell, giving it an increased moment arm, and hence greatly increasing the stiffness, so that when the prestressed shell is released, it coils only imperceptibly. Flattening the corrugations reduces the stiffness of the shell down to that of an uncorrugated sheet, and so, under the prestress, it coils up much more.

Note that multistable shells are possible without prestress, even in isotropic shells; see Seffen<sup>6</sup> for one possible example. The critical issue is that, since the internal stresses can be assumed to be linearly elastic,

any distortion mechanism in which the force-displacement curve is also linear (i.e. the stiffness is constant over large deflections) will provide only one equilibrium solution. Therefore, multistability can only arise where, due (for example) to geometrical effects, the force-displacement curve is nonlinear.

## II.B. The method of construction

If a multistable shell is not prestressed, construction is a straightforward matter of pressing or otherwise forming the desired shape. However, if prestresses must be built in, the shell is first pressed into the shape into which the prestresses (when released) deform it. The structure is then deformed plastically to create the new shape; this deformation will affect the prestresses, but not remove them.

When we construct our prototypes, this final plastic deformation must be performed cold, so as to preserve the residual stresses. Most prototypes were formed from a Copper-Beryllium alloy, chosen for its high yield strain; shim steel has also been used successfully.

## III. Analytical modelling

**S**IMPLE analysis is needed to explain the observed behaviour in a way consistent with general elastic theory. Here, we set up two simple elastic models which take what we believe to be the starting conditions for bistability, and then evaluate the internal energy as the shape of the shell varies. We expect to see local energy minima corresponding to the stable shapes observed.

The following models do not consider the method by which the shells are formed. We have found both upper-bound and lower-bound analyses to be inadequate to predict the final behaviour from the forming process (or, in similar fashion, to specify the forming process for a desired final behaviour), and have therefore produced a plastic flow model, assuming an Elastic-Perfectly Plastic (EPP) material that yields to a Tresca criterion. This plastic flow model has provided a useful insight into the formation process and the resulting internal stresses, but they are not part of the subject of this paper: see Norman's first year PhD report.<sup>7</sup>

It is trivial to combine the two models here to describe tristable shells, which we leave to the reader.

### III.A. Elastic principles

Definitions of curvature are identical to those of Calladine.<sup>1</sup> This analysis assumes that the material is linear-elastic, obeying Hooke's law with a Young's modulus  $E$  and a Poisson's ratio  $\nu$ . Since the shell is thin, plane stress behaviour can be assumed. Accordingly, Calladine<sup>1</sup> assembles the following generalised Hooke's law for an *isotropic* shell in bending (for anisotropic materials, the bending stiffness matrix  $\mathbf{D}$  changes);

$$\begin{bmatrix} M_{xx} - M_{xx_0} \\ M_{yy} - M_{yy_0} \\ M_{xy} - M_{xy_0} \end{bmatrix} = \mathbf{M} - \mathbf{M}_0 = \mathbf{D}(\boldsymbol{\kappa} - \boldsymbol{\kappa}_0) = D \begin{bmatrix} 1 & \nu & 0 \\ \nu & 1 & 0 \\ 0 & 0 & \frac{1-\nu}{2} \end{bmatrix} \begin{bmatrix} \kappa_{xx} - \kappa_{xx_0} \\ \kappa_{yy} - \kappa_{yy_0} \\ 2(\kappa_{xy} - \kappa_{xy_0}) \end{bmatrix} \quad (1)$$

where  $D$  is the shell bending stiffness, defined by

$$D = \frac{Et^3}{12(1-\nu^2)} \quad (2)$$

Defining the change in curvature  $\mathbf{k} = \boldsymbol{\kappa} - \boldsymbol{\kappa}_0$ , the elastic strain energy density at a given point for a given state is the integral of the work done  $\mathbf{M}^T \mathbf{k}$  over deformation from the initial state to that state. This is a conservative system, and therefore history-independent; the energy density  $U$  relative to the initial state  $\boldsymbol{\kappa}_0$ ,  $\mathbf{M}_0$  is

$$U = \frac{1}{2} \mathbf{k}^T \mathbf{D} \mathbf{k} + \mathbf{M}_0^T \mathbf{k} \quad (3)$$

Remember that  $\mathbf{D}$  can be a general anisotropic matrix, over and above the isotropic form.

One condition of stability is that the equilibrium states have positive stiffness, thereby equating to local energy minima. This can be expanded into two specific criteria;

1. for equilibrium, there must be no mechanism driving the system in any direction; therefore, the local energy gradient (partial derivatives with respect to any shape factors) must be zero, and

2. for stability, the stiffness matrix must be positive definite at that point, so that any small deformation will place the structure in a state from which it has a direct mechanism back to the previous form.

Equilibrium points which do not fulfil the second criteria come in three forms:

1. maxima, with all second-order derivatives zero or negative: they are unstable, and the structure may deform in any direction;
2. saddle points with some negative second-order derivatives and some positive, which are unstable only in one direction, and stable in orthogonal directions;
3. metastable points: the second derivatives are zero in all directions, and the structure has zero stiffness.

This can all be determined analytically. However, once the equilibrium points are found, it is quicker to examine a contour plot of energy to determine whether they are minima, maxima, saddles or metastable.

### III.B. The elastic properties of corrugated sheets

The fundamental concept used to simplify the problem is the distinction between two scales: a ‘global’ scale, in which the corrugated sheet is rendered as a flat or developable sheet with anisotropic properties, and the ‘local’ scale within the corrugations, where the sheet is isotropic. While a global curvature along the corrugations will produce local tensions & strains, the strain energy within the sheet due to these strains is the same as the purely bending strain energy of the anisotropic global sheet, and the complex problem of non-zero Gaussian curvature on the local scale is turned into the simpler problem of developable curvature on the global scale. Only changes to the corrugation profile itself need be considered at the local scale, and this is, again, purely a bending effect. No net tension or compression is applied to the shells in these analyses.

The bending stiffness of the corrugated sheet in the  $y$  direction is the same as the local value  $D$ . In addition, the global twisting stiffness takes the local value  $(1 - \nu)D/2$  and the Poisson coupling of curvature in the  $x$  and  $y$  directions remains at  $\nu D$ , as for the isotropic sheet. Only the bending stiffness along the corrugations is affected by the presence of the corrugations. In that direction, the local stiffness  $D$  is augmented by the moment-arm of the material about the central plane, giving an additional stiffness  $\alpha D$ , where  $\alpha$  is a function of the shape of the corrugations. This gives a new stiffness matrix

$$\mathbf{D} = \begin{bmatrix} (1 + \alpha)D & \nu D & 0 \\ \nu D & D & 0 \\ 0 & 0 & \frac{1-\nu}{2}D \end{bmatrix} \quad (4)$$

If we were to consider stretching of the global sheet, we would have to develop a much more sophisticated model, since (for a corrugated sheet) stretching across the corrugations has a significant effect on bending stiffness along them.

### III.C. Elastic model 1: coiling bistability

This model deals purely with the behaviour of a flat corrugated sheet in which prestress tends to coil it up, and does not consider twist deformation. A sheet is modelled as having corrugations that run parallel to the  $x$  axis of the sheet. These corrugations are taken to be composed of alternating circular arcs, curving in the  $y$  direction.

#### III.C.1. Equations

Figure 4 shows a section from a corrugated sheet in which edge effects are neglected. This figure shows simultaneously the  $y$ -direction corrugation curvature of the corrugated mode and the global  $x$ -direction curvature of the coiled mode, although we expect to find that the stable states have just one or the other present with non-negligible magnitude. The global curvature in the  $x$  direction is defined as  $k$ . The corrugation curvature varies in the  $y$  direction, and is termed  $c(y)$ .

The initial state is taken to be the corrugated mode ( $k = 0$ ), and the corrugation takes some initial value  $c_0(y)$ . There is a prestress moment  $M$  purely in the direction of the corrugations. From this initial state,

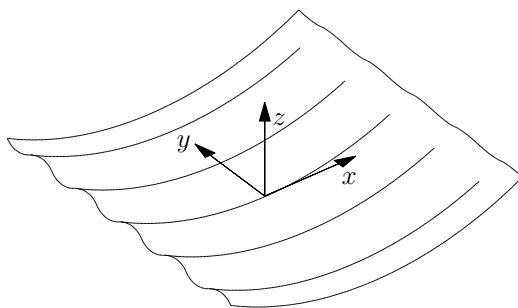


Figure 4: The 1-dimensional curvature model.

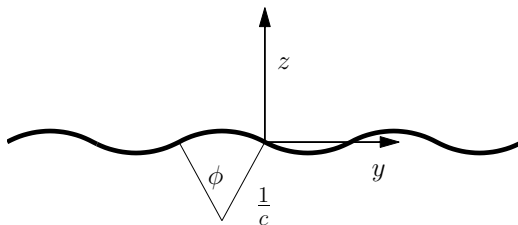


Figure 5: The circular-arc corrugation profile.

assume that the corrugation curvature  $c(y)$  is related to the initial curvature  $c_0(y)$  by  $c(y) = \beta c_0(y)$ , where  $\beta$  is a spatially-constant scalar coefficient; the initial corrugated shell has  $\beta = 1$ , and once the corrugations have been flattened and the sheet coils up,  $\beta = 0$ . Then, the initial prestress moments  $M_{ij_0}$ , initial curvatures  $\kappa_{ij_0}$  and subsequent curvature changes  $\Delta\kappa_{ij}$  are

$$\begin{array}{lll}
 M_{xx_0} = M & \kappa_{xx_0} = 0 & \Delta\kappa_{xx} = k \\
 M_{yy_0} = 0 & \kappa_{yy_0} = c_0(y) & \Delta\kappa_{yy} = c(y) = (1 - \beta)c_0(y) \\
 M_{xy_0} = 0 & \kappa_{xy_0} = 0 & \Delta\kappa_{xy} = 0
 \end{array} \tag{5}$$

Substituting these curvatures and prestress moments into Equation 3 gives a strain energy density equation that varies with  $y$ :

$$U(y) = Mk + \frac{1}{2}D \left\{ (1 + \alpha)k^2 + 2\nu k(1 - \beta)c_0(y) + [(1 - \beta)c_0(y)]^2 \right\} \tag{6}$$

The corrugation curvatures are a pattern which repeats every wavelength  $\lambda$ . So, the average curvature of the shell in the  $y$  direction is the integral of  $c(y)$  from  $y = 0$  to  $y = \lambda$ , all divided by  $\lambda$ . However, we have stipulated that the sheet has no global curvature in the  $y$  direction in the initial state, so

$$\frac{1}{\lambda} \int_0^\lambda c_0(y) dy = 0 \tag{7}$$

Thus, we can simplify Equation 6 to give the average strain energy density  $\bar{U}$ :

$$\bar{U} = \frac{1}{\lambda} \int_0^\lambda U(y) dy = Mk + \frac{1}{2}D \left[ (1 + \alpha)k^2 + \frac{(1 - \beta)^2}{\lambda} \int_0^\lambda c_0^2(y) dy \right] \tag{8}$$

Note that this energy equation separates global-curvature  $k$  terms from local  $c$  terms.

It remains to define  $\alpha$ . If we consider each element of length  $dy$  and material depth  $t$  to be a distance  $a$  from the centreplane of the corrugations, then

$$\alpha D = \frac{1}{\lambda} \int_0^\lambda Ea^2 t dy \tag{9}$$

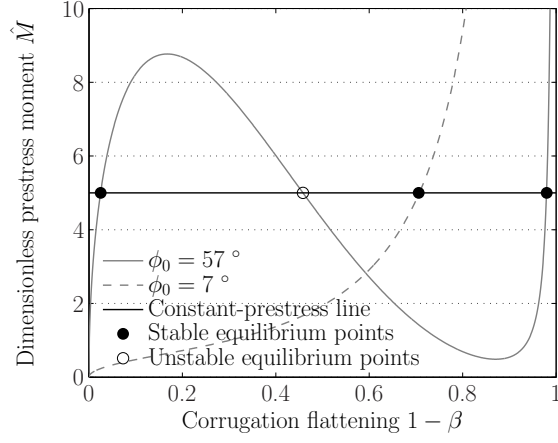


Figure 6: Equilibrium plot of moment  $\hat{M}$  against corrugation flattening  $1 - \beta$  at  $\hat{c}_0 = 0.00625$ . The gradient of the equilibrium curve is the stiffness of the shell in flattening, so positive gradient = positive stiffness (stable) and negative gradient = unstable. A given prestressed shell has a constant  $\hat{M}$  (in this example, 5). Where the line of constant  $\hat{M}$  crosses the equilibrium curve, there is an equilibrium point. Below  $\phi_0 = 14^\circ$ , the unstable region vanishes and the structure becomes monostable.

Our corrugation profile is shown by Figure 5, consisting of a series of alternating circular arcs of subtended angle  $\phi$  and curvature  $c$ , so  $c(y)^2 = c = \text{constant}$  and  $\lambda = 2\phi/c = 2\phi_0/c_0$ . At this point, the following dimensionless variables are introduced for compactness:

$$\hat{c}_0 = c_0 t \quad \beta = \frac{c}{c_0} \quad \hat{k} = \frac{k}{c_0} \quad \hat{M} = -\frac{M}{Dc_0} \quad \hat{U} = \frac{\bar{U}}{\frac{1}{2}Dc_0^2} \quad (10)$$

Substituting the curvature profile into Equation 8 and rearranging it into dimensionless form,

$$\hat{U} = \hat{k}^2(1 + \alpha) + (\beta - 1)^2 - 2\hat{M}\hat{k} \quad (11)$$

and from Figure 5 & Equation 9, we can (through intervening steps) determine that

$$\alpha = \frac{12(1 - \nu^2)}{\hat{c}_0^2} \left[ 1 + \frac{1}{2} \cos(\beta\phi_0) - \frac{3}{2\beta\phi_0} \sin(\beta\phi_0) \right] \quad (12)$$

Equilibria are formally obtained by setting  $d\hat{U}/d\hat{k} = d\hat{U}/d\beta = 0$ , giving equations for equilibrium values:

$$\hat{k} = \frac{\hat{M}}{1 + \alpha} \quad (13)$$

$$\hat{U} = (\beta - 1)^2 - \frac{\hat{M}^2}{1 + \alpha} \quad (14)$$

$$\hat{M} = (1 + \alpha) \sqrt{2(1 - \beta) \frac{d\beta}{d\alpha}} \quad (15)$$

$$\frac{d\alpha}{d\beta} = \frac{12(1 - \nu^2)}{\hat{c}_0^2} \left[ \frac{3}{2\phi_0\beta^2} \sin(\beta\phi_0) - \frac{3}{2\beta} \cos(\beta\phi_0) - \frac{\phi_0}{2} \sin(\beta\phi_0) \right] \quad (16)$$

With Equations 13 to 16, we can now describe the behaviour of the global and local curvature of the sheet under any moment  $\hat{M}$ .

### III.C.2. Behaviour

Figure 6 plots Equation 15, showing the equilibrium prestress moment  $\hat{M}$  related to the corrugation curvature  $\beta$ , for  $\hat{c}_0 = 0.00625$  (chosen to match the shells we produced). It is a plot of moment against shell flattening;

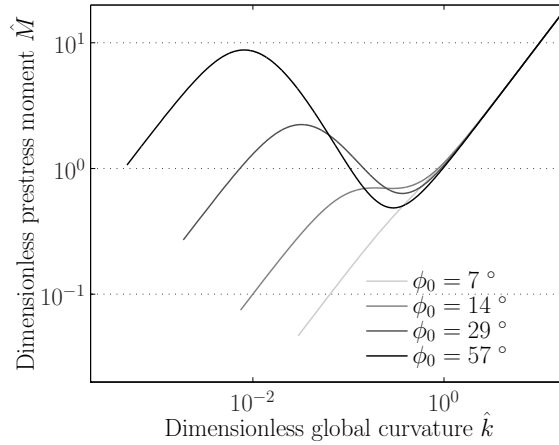


Figure 7: Log-log equilibrium plot of moment  $\hat{M}$  against global curvature  $\hat{k}$  at  $\hat{c}_0 = 0.00625$ . Again, a given shell has a constant moment  $\hat{M}$ , and the equilibrium points for the shell are where the constant- $\hat{M}$  line crosses the equilibrium curve. This shows clearly the linear-elastic nature of the stable regimes, with the second stable state corresponding to the linear stiffness of an uncorrugated sheet.

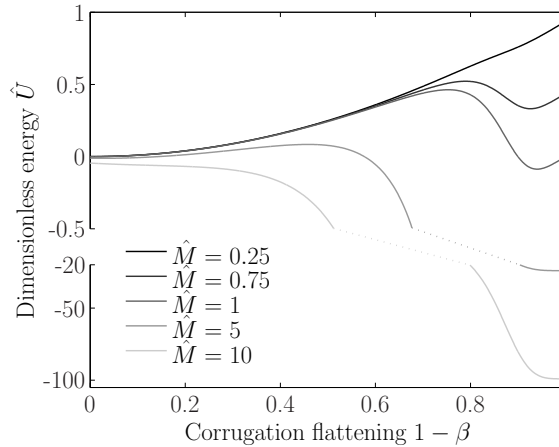


Figure 8: Plot of energy density  $\hat{U}$  against corrugation flattening  $1 - \beta$  at  $\hat{c}_0 = 0.00625$  and  $\phi_0 = 57^\circ$  for various moments  $\hat{M}$ . A large section of the  $\hat{U}$  axis has been cut out so as to give detail around  $\hat{U} = 0$  whilst showing features down to  $\hat{U} = -100$ . At higher  $\hat{M}$ , the coiled mode ( $\beta$  small) is lower-energy; at lower  $\hat{M}$ , the corrugated mode is lower-energy. For very large or small  $\hat{M}$ , the bistability vanishes.

its gradient is the flattening stiffness of the shell in response to an applied moment. There are two regions of positive gradient, i.e. positive stiffness, and one region between of negative stiffness.

For a given shell,  $\hat{M}$  will be fixed; so, where the line of constant  $\hat{M}$  crosses the equilibrium curve for a given shell, that shell is in equilibrium. For a range of values of  $\hat{M}$  for  $\phi_0 \geq 0.25$ , there are three solutions for a given moment. Two of these lie on regions of positive gradient, have positive stiffness and are therefore stable. The point in between has negative stiffness, and hence is unstable, and so these shells are bistable. This is expected; for a reasonable corrugation depth, certain moments allow bistability. If the prestress moment is too low, there is no stable coiled mode (at low  $\beta$ ); if the prestress is too high, there will be no stable corrugated mode (at high  $\beta$ ). In addition, as  $\phi_0$  becomes small, the corrugations tend to a flat sheet, which is not bistable. The section of negative stiffness between the stable points demonstrates that there is no stable equilibrium solution for a path between the stable points.

Figure 7 shows the same data but plots  $\hat{M}$  against global curvature  $\hat{k}$ . This is the moment-curvature response of the shell, and its gradient is the bending stiffness of the shell. It can be seen that the corrugated



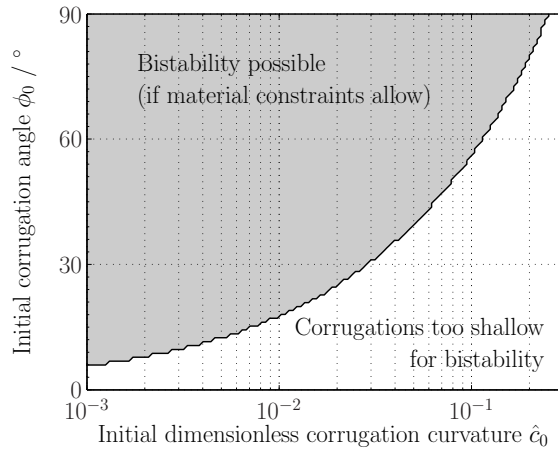


Figure 9: As Figures 6-7 show, when the corrugations are too small (i.e. the curvature  $\hat{c}_0$  is too tight or the subtended angle  $\phi_0$  is too small) bistability is not possible.

stable form has very low global curvature. In the coiled mode, the moment-curvature relationship becomes linear with gradient  $D$ , or 1 in our dimensionless form.

For bistable shells, if the shell is held such that it is half coiled and half corrugated, one of these states may have lower energy, in which case the transition region between them will move to the opposite end and the shell will globally take on the lower energy state. Figure 8 shows the internal strain energy variation with  $\beta$  for a range of moments at  $\phi_0 = 29^\circ$ ; note how at low moments, the corrugated state has lower energy, and for high moments, the coiled state. There is, therefore, one moment at which both states have the same energy, and therefore any half-transformed shell will rest without becoming fully corrugated or fully coiled; it is ‘neutrally stable’, with no energy gradient in either direction. In Figure 8, this is at  $\hat{M} = 0.88$ .

In summary, Figure 9 shows the bistable region in  $\beta$ - $\phi$  space. This provides a general design guide for the bistable shells.

### III.D. Elastic model 2: twisting bistability

This model predicts the twisting bistability. The same hierarchical model (‘global’ and ‘local’) is used as in Section III.C, with corrugations and prestress in the  $x$  direction. However, there are two changes to the model:

1. The corrugations are not permitted to flatten or buckle, i.e.  $\beta = 1$  at all times, which accords with observations;
2. Global curvature is no longer purely in the  $x$  direction; the global curvature  $k$  is applied at an angle  $\theta$  to the  $x$  axis (as shown in Figure 10), beginning at an initial (formed) value  $k_0$  at  $\theta = 90^\circ$ .

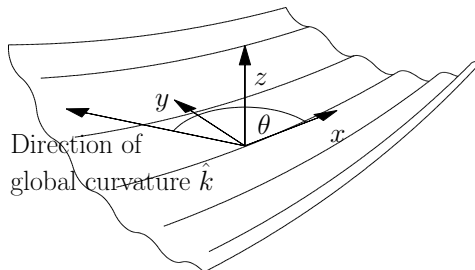


Figure 10: The 2-dimensional curvature model, with global curvature  $k$  at an angle  $\theta$  to the  $x$  axis.

### III.D.1. Equations

The curvature changes are derived from Mohr's circle of strain, as in Guest & Pellegrino:<sup>3</sup>

$$\Delta\kappa_{xx} = \frac{1}{2}k(1 + \cos 2\theta) \quad \Delta\kappa_{yy} = \frac{1}{2}k(1 - \cos 2\theta) - k_0 \quad \Delta\kappa_{xy} = -\frac{1}{2}k \sin 2\theta \quad (17)$$

and it is convenient to make variables dimensionless against the initial curvature  $k_0$  rather than  $c_0$ , so

$$\hat{k} = \frac{k}{k_0} \quad \hat{M} = -\frac{M}{Dk_0} \quad \hat{U} = \frac{\bar{U}}{\frac{1}{2}Dk_0^2} \quad (18)$$

Substituting the  $\Delta\kappa$  values of Equation 17 into Equation 3,

$$\hat{U} = \hat{k}^2 \left[ 1 + \frac{\alpha}{8} (3 + 4 \cos 2\theta + \cos 4\theta) \right] + \hat{k} [(1 - \nu) \cos 2\theta - (1 + \nu)] + 1 - \hat{M}\hat{k}(1 + \cos 2\theta) \quad (19)$$

Equilibrium configurations are those that satisfy  $d\hat{U}/d\theta = 0$  and  $d\hat{U}/d\hat{k} = 0$ . The solutions to these equations are:

1.  $\hat{k} = 0$ ,  $\cos 2\theta = \frac{1+\nu+\hat{M}}{1-\nu-\hat{M}}$ , if  $\hat{M} < -\nu$ . This is not a stable solution, i.e. not a minimum;
2.  $\hat{k} = 1$ ,  $\theta = 90^\circ$ . This is the initial state, is an equilibrium point for all cases, and is stable when  $\hat{M} < 1 - \nu$  (else, it is a saddle point);
3.  $\hat{k} = 1$ ,  $\cos 2\theta = \frac{1+\nu+\hat{M}}{1-\nu-\hat{M}}$ . This solution only exists for  $1 - \nu < \hat{M} < \alpha + 1 - \nu$ , but is always stable. Note that since  $\cos 2\theta$  is a symmetric function, there is a symmetric pair of stable solutions;
4.  $\hat{k} = \frac{\hat{M}+\nu}{\alpha+1}$ ,  $\theta = 0$ . This always exists, but is only stable when  $\hat{M} > \alpha + 1 - \nu$ , being otherwise a saddle point.

The minima are easiest understood from a contour plot of energy, where minima denote stable points. The two variables controlling the shape of the sheet are curvature magnitude and direction, and so a polar plot makes the most sense; thus, distance from the origin denotes tightness of curvature (so at the origin, the sheet is flat). Angle on the plot, however, denotes  $2\theta$  rather than  $\theta$ , because a polar plot contains  $360^\circ$  but curvature repeats every  $180^\circ$ . Figure 11a shows the plot coordinates.

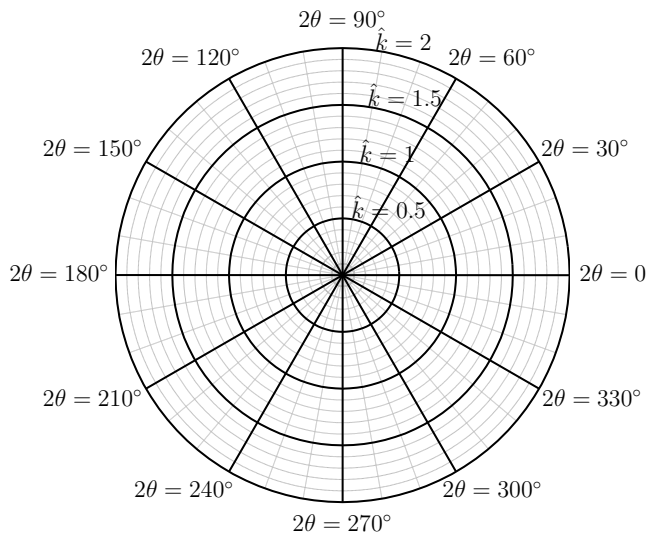
### III.D.2. Behaviour

From the enumerated solutions above, there are three distinct modes of operation in which the stable points are located by different equations. The bistable mode is found as solution 3, where  $\hat{M}$  lies in the range

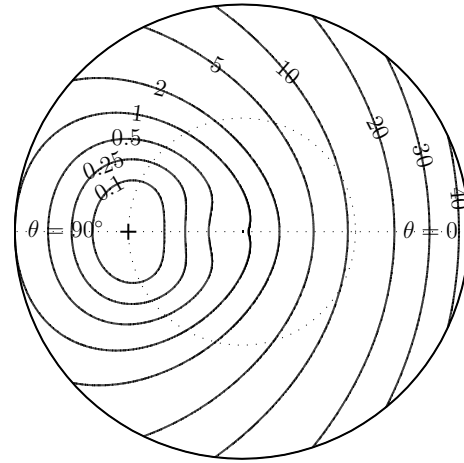
$$1 - \nu < \hat{M} < \alpha + 1 - \nu \quad (20)$$

and only this range of prestress moments will provide bistability. Otherwise, there is just one stable point at either  $\theta = 0$  (solution 2, the initial state, when the prestress is small or negative) or  $\theta = 90^\circ$  (solution 4, for very large prestress). Figure 12 shows this condition graphically in  $\alpha$ - $\hat{M}$  space; all cases of a corrugated material with a positive, non-zero  $\hat{k}_0$  can be placed on this plot. Negative  $\hat{k}_0$  values may produce bistability, but they do not produce the twist mode, and are not of interest here. They produce similar effects to those described by Kebabze et. al.<sup>5</sup> of a shell given two conflicting curvatures of perpendicular orientations of opposite sense, which are the two stable states. Figure 11 shows all of the behaviour discussed here, giving contour plots of internal strain energy for a variety of prestress moments.

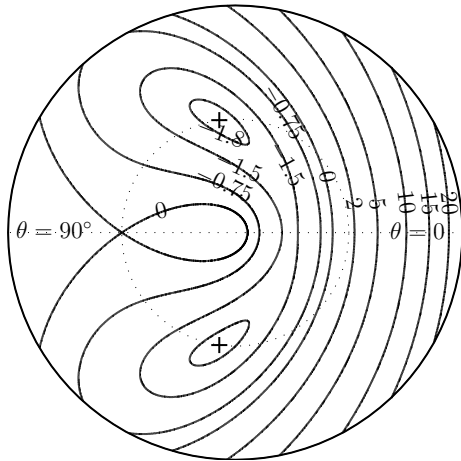
We have shown that the observed twisting behaviour can arise from the interaction between an initial curvature across the corrugations and a prestress moment along them. Equally, this can be seen as the result of two conflicting prestresses, and only arises when one prestress is not too much greater than the other; producing a two-dimensional prestress moment ( $M_{xx} \neq 0$ ,  $M_{yy} \neq 0$ ,  $M_{xy} = 0$ ) with  $\kappa_0 = 0$  gives the same behaviour. Without the corrugations (i.e. in isotropic shells,  $\alpha = 0$ ), the range in Equation 20 vanishes,  $\theta_M$  becomes indeterminate and the twisting bistability becomes impossible to create. Note also that, as long as  $\alpha$  is correctly calculated, this behaviour is completely independent of the corrugation profile, and if  $\alpha$  is unaffected, triangular, sinusoidal, circular-arc or any other corrugation will behave identically. This is *not* true of the 1-dimensional model in Section III.C.



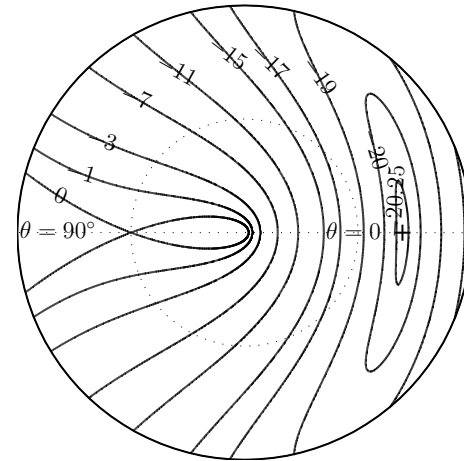
(a)  $(\kappa, 2\theta)$  polar grid definition.



(b) Monostable:  $\hat{M}$  is too small for bistability, and the one stable point is at  $\hat{k}_M = 1$ ,  $\theta_M = 90^\circ$ . There is a small saddle point at  $\hat{k} = 0$ .  $\alpha = 10$



(c) Intermediate moments; two stable states at  $\hat{k}_M = 1$ , at angle  $\pm\theta_M$  given by  $\cos 2\theta_M = 2(\hat{M} - 1 + \nu)/\alpha - 1$ . Here,  $\hat{M} = 5$ ,  $\alpha = 10$ . There are saddle points on  $\theta = 90^\circ$  (at  $\hat{k} = 1$ ) and on  $\theta = 0$ .



(d)  $\hat{M}$  has here been increased to 15, and bistability disappears. Now,  $\theta_M = 0$ ,  $\hat{k}_M > 1$ .

Figure 11: Energy-density contours for the two-dimensional model. Figure 11a gives the  $(\kappa, 2\theta)$  polar grid definition for these plots. Contours are of energy  $\hat{U}$ .  $\nu = 0.3$  throughout.  $\alpha = 10$  corresponds to  $\phi = 15^\circ$ , and  $\alpha = 145$  to  $\phi = 30^\circ$ . Crosses denote stable points (minima). Note that the  $\hat{U} = 0$  contour crossing its own path in Figures 11c & 11d denotes a saddle point.

## IV. Conclusions

UNIFORM corrugated shells can be manufactured which are bistable in either or both of two modes: a corrugated sheet coils up when the corrugations are flattened, and a corrugated sheet which, in addition to curvatures along and perpendicular to the corrugations, has a ‘twist’ which is stable at both its positive and negative value. When these modes are combined in one shell, that shell is tristable. In both modes, multistability arises due to a ‘prestress’, i.e. a residual bending moment in the shell in the initial corrugated state which interacts with nonlinear geometry changes. We set up an elastic model and evaluated the strain

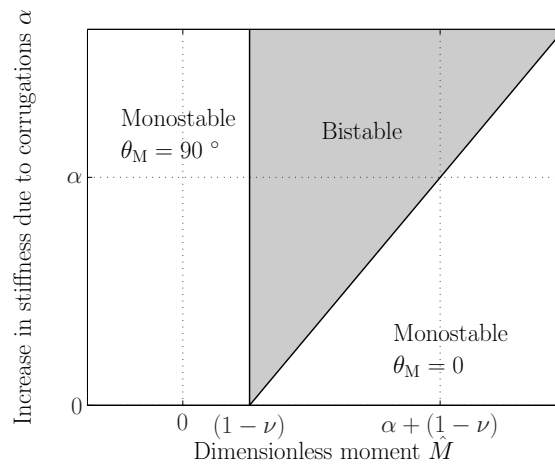


Figure 12: A ‘design chart’ for twist bistability, showing the range of values of  $\hat{M}$  for bistability as a function of  $\alpha$ . Subscript M denotes minimum-energy states, i.e. stable equilibria.

energy density in this model as the shape is changed, in order to determine the stable shapes. Despite very simple assumptions of internal stresses, we have produced non-trivial results which reproduced a number of details of the behaviour of the prototypes. Furthermore, having produced these models, they have been sufficiently useful to guide our construction of prototypes, teaching us how to avoid or enforce specific modes of behaviour, and how to tailor the properties of the shells to suit the situation for which they are intended, which is the goal of shell-structure engineering.

## V. Ongoing & future work and applications

A patent has been filed for this technology,<sup>8</sup> and we are actively pursuing applications, including a backing for flexible display screens and other deployable electronic devices (e.g. keyboards). Other long-term concepts include deployable/adaptive wings/panels for small-scale (e.g. unmanned) aircraft and spacecraft.

We have also joined coiling sheets in layers, creating sheets which, when in their flat state, have a honeycomb-type section, but which can still coil up. This greatly increases the stiffness of the structure, and produces an enclosed hollow section in which anything from wires to fuel can be placed and protected.

All of the analyses above assume shells whose geometric and structural properties are uniform. However, most structures do not experience completely uniform conditions; they have complex shapes and localised loadings, and a non-uniform solution can therefore be much more effective and efficient than a uniform one. For this reason, our current research is exploring more complex shapes. As the shells become more complex in shape, so the opportunities expand for elastic shape-change with multiple stable states.

## References

- <sup>1</sup>Calladine, C. R., *Theory of Shell Structures*, Cambridge University Press, 1983, ISBN 0521238358.
- <sup>2</sup>Hyer, M. W., “Calculations of the room-temperature shapes of unsymmetric laminates,” *Journal of Composite Materials*, Vol. 15, July 1981, pp. 296–310.
- <sup>3</sup>Guest, S. D. and Pellegrino, S., “Analytical models for bistable cylindrical shells,” *Proceedings of the Royal Society A: Mathematical, Physical and Engineering Sciences*, Vol. 462, No. 2067, March 2006, pp. 839–854.
- <sup>4</sup>Galletly, D. A. and Guest, S. D., “Bistable composite slit tubes. I. A beam model,” *International Journal of Solids and Structures*, Vol. 41, No. 16-17, Aug. 2004, pp. 4517–4533.
- <sup>5</sup>Kebadze, E., Guest, S. D., and Pellegrino, S., “Bistable prestressed shell structures,” *International Journal of Solids and Structures*, Vol. 41, No. 11-12, June 2004, pp. 2801–2820.
- <sup>6</sup>Seffen, K. A., “Mechanical memory metal: a novel material for developing morphing engineering structures,” *Scripta Materialia*, Vol. 55, No. 4, Aug. 2006, pp. 411–414.
- <sup>7</sup>Norman, A. D., *Analysis & design of multistable corrugated open shell structures*, First-year PhD report, Cambridge University, Aug. 2006.
- <sup>8</sup>Seffen, K. A., Guest, S. D., and Norman, A. D., “Multistable Structural Member And Method For Forming A Multistable Structural Member,” Patent Pending, July 2006, GB 0612558.7.